Obstacle detection system for autonomous vineyard robots based on passthrough filter

Weixu Ran[1], Yubin Lan[1,2], Xianglong Dai[1], Jian Gu[1], Baixu Liu[1], Lijie Geng[1], Xin Han[1], Lili Yi[1*]

(1. *College of Agricultural Engineering and Food Science, Shandong University of Technology, Shandong Provincial Engineering Technology Research Center for Agricultural Aviation Intelligent Equipment, Zibo 255022, Shandong, China*; 2. *Zibo Agricultural and Rural Service Center, Zibo 255022, Shandong, China*)

Abstract: This research aims to solve an obstacle detection problem to enable safety autonomous robot to work in complex vineyard environments. The problem remains challenging because paths planning to avoid obstacles discovered by onboard 3D LiDAR requires creating and updating a representation of the environment that can be searched by feasible paths. The process is computationally expensive. In this paper, we proposed a passthrough filter based obstacle detection solution in the robot operation system (ROS) architecture without increasing the hardware burden. In this solution, 3D LiDAR mounted on the robot was used to do the tree-row followed navigation and the obstacles detection in different ROS function packages with different point cloud processing. In the proposed solution, the range of interest (ROI) to detect the obstacle can be set by the user interface. The ROI is 0.7 m to 6m in front of the robot header. To verify the proposed solution, different types of obstacles including static small things like boxes, static big items like another robot and moving person were detected in field experiments. Experiments demonstrated that the proposed solution could detected obstacles in determined ROI successfully with low computational cost as 10 ms.

Keywords: autonomous robot, 3D LiDAR, obstacle detection, obstacle Estimation

DOI: 10.33440/j.ijpaa.20220501.192

Citation: Ran W X, Lan Y B, Dai X L, Gu J, Liu B Y, Geng L J, Han X and Yi L L. Obstacle detection system for autonomous vineyard robots based on passthrough filter. Int J Precis Agric Aviat, 2022; 5(1): 41–46.

1 Introduction

Orchards management requires a great deal of maintenance throughout the year, pruning, bloom thinning, spraying for insects and disease, and mowing the grass between the trees[1]. These activities make up a significant portion of operating expenses and improvements in efficiency can directly improve a vineyards productivity. More and more professional farmers recognize the potential of automation to reduce chemical exposure to their employees during spraying and help reduce the logistical difficulties of finding sufficient, skilled, seasonal labor.

Recent years, autonomous agriculture equipment has become more and more feasible with the development of navigation technologies including Micro-Electro-Mechanical System (MEMS), Global Navigation Satellite System (GNSS), Artificial Intelligence (AI) and so on. The GNSS receiver with multi-system, multi-band and Real-time Kinematic (RTK) can improve the positioning accuracy to be several centimeters in the open field[2-10]. Except that, the cost of the GNSS-RTK system is lower and lower with the development of network RTK. Consequently, many researchers put their attention on autonomous agriculture vehicles, especially on precision localization and automatic guidance.

However, the limitation of GNSS-RTK is also introduced huge positioning errors in Non-Line-of-Sight (NLOS) environments since of the refraction and diffraction during the satellite signal propagation, such as in the orchards and during cloudy days. For example, in mixed LOS/NLOS environments, the accuracy of the GNSS-RTK system will decreases from 5cm to 10 meters even to 100 meters[7-10]. Spatial information collected by Inertial Measurement Unit (IMU), 3D LiDAR and RGB-D camera is required to localize the agricultural vehicles as accurate as possible[11-13]. Except that, the point cloud image or the visual image also can be used to recognize the obstacles among the front view of the sensors. In the past several years, a lot of research work published on the CVPR have focused on the point cloud-based target recognition and target tracking.

In the year of 2021, we also proposed a tree followed navigation algorithm-based vineyard robot named SDUT-PAART-1.

On most scenarios, SDUT-PAART-1 working in vineyards use along the planted tree row and turning around at the end of tree row. From the kinematics point of view, it can be decomposed as constant velocity (CV) and constant turning (CT) movement in the vineyard. For constant velocity movement, autonomous row following has become a popular research area especially in

Received date: 2022-11-15 **Accepted date:** 2022-12-05

Biographies: Weixu Ran, postgraduate, research interests: agricultural automation, Email: 625973407@qq.com; **Yubin Lan**, PhD, Distinguished Professor, Director, research interests: precision agricultural aviation application, Mailing Address: College of Electronic Engineering, South China Agricultural University. Email: ylan@scau.edu.cn; **Xianglong Dai**, research interests：orchard autonomous navigation, Emile: 1047850171@qq.com; **Jian Gu**, research interest：simultaneous localization and mapping, Email: gujian0705@163.com; **Baixu Liu**, research interests; automatic driving planning control, Emile: 2541252346@qq.com; **Baixu Liu**, research interests;Automatic driving planning control, Emile: 2541252346@qq.com; **Lijie Geng**, postgraduate, research interests: agricultural automation, Email: 1779333079@qq.com; **Xin Han**, Professor, research interests: agricultural aerial application technology, Email: hanxin@sdut.edu.cn;

***Corresponding author: Lili Yi,** PhD, research interests: agricultural automation and autonomy. Room 6-915, School of Agricultural Engineering and Food Science, Shandong University of Technology, Zibo 255000, China. Tel: +86-18369916558, Email: yili0001@sdut.edu.cn.

agriculture application because of the standardized planting model[9-18]. The task consists of detecting a pathway for an agriculture vehicle to follow, using environmental sensors including 3D LiDAR, IMU and camera.

Typically, the path planning problem with obstacle recognition is broken down into two subproblems. The first one solves a global planning problem possible assisted by heuristic to ensure the path does not fall into local minima. The second one solves a local planning problem that runs in parallel to track the global path as well as avoid obstacles. This method has been adopted successfully in autonomous navigation application shown in citation[1-3].

Based on these previously knowledge, an orchard used moving robot is designed and implemented in the year of 2020 and related research work is shown in details in the paper proposed by our research team[20]. However, the application of the moving robot only considered the dynamic models of the robot without proposing the obstacles on the way of the robot. To overcome this weakness, we purposed our research to incorporate the obstacle detection algorithm into the robot to make sure it can move in the orchards safely without any traffic accidents.

In this paper, we address the problem of obstacle detection algorithm for autonomous orchard vehicles moving at a speed of less than 1 m/s using only a 64-channel 3D LiDAR. Our algorithm consists different steps summarized as follows. First the 3D point cloud is registered to the vehicle and inertial coordinate frame. Then the registered point cloud is downgraded to be simple grid map with position information of the interested obstacles. Finally, obstacles in the range of interest (ROI) are recognized with distance to the moving robot. Passthrough filter is employed to filter out obstacles in the ROI.

The rest of the paper is organized as follows. Section 2 describes the. Section 3 describes the passthrough filter based obstacle detection system implemented separately with Raspberry PI to verify the ideas and to verify the computational cost. Section 4 describes all the experiments implemented in the vineyard and evaluated the experiments results. Section 5 draws the conclusion of this paper.

2 Materials and methods

To implement and verify the proposed obstacle detection system, two sets of hardware is employed. In the very beginning, a Raspberry PI and 3D-LiDAR based embedded system was constructed to verify the proposed ideas under indoor environment using c++ without ROS. After that, a Jetson AGX based processing system was constructed together with the tree row followed navigation algorithm in the ROS architecture.

2.1 Raspberry PI based system

An experiment obstacle detection embedded system named RPS included the main processer Raspberry PI and the 32-channel 3D-LiDAR.

As shown in Figure 1, the RPS can detect 3 different ROI regions which can be configured by a Linux script file. The ROI is denoted as

$$R\_r_k=S(R\_x_k,\mathrm{R}\_y_k) \quad (1)$$

$$Y\_r_k=S(Y\_x_k,\mathrm{Y}\_y_k) \quad (2)$$

$$G\_r_k=S(G\_x_k,\mathrm{G}\_y_k) \quad (3)$$

where r_k stands for the ROI, (x_k,y_k) stands for the valid position in the local coordinate. Configuration file is shown in Figure 2. To successfully configure the RPS, we should make sure that R_r_k is smaller than Y_r_k and Y_r_k is smaller than G_r_k. Parameter configuration example is shown in Figure 2.

Table 1 Detailed information of the RPS platform

	Parameter	Value
Lidar	Precision	±0.7-5 cm
	Frequency	10 Hz
	Detection distance	120 m
	Horizontal resolution	1024
Raspberry PI	SOC	Broadcom, BCM2837B0
	CPU	64-bits, 1.4 GHz
	GPU	Broadcom, VideoCore@400MHz
	Memory	8G
Connector	USB2.0	4
	Ethernet	1000M
	Wifi	5 GHz

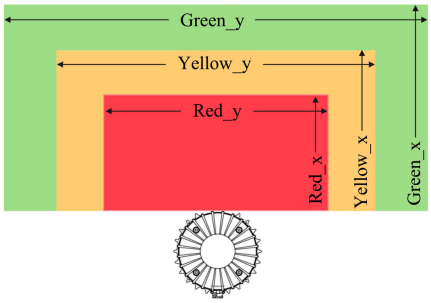

Figure 1 ROI of the RPS platform with Raspberry PI and 3D-LiDAR, Red range stands for the nearest region while the green part stands for the largest region

parameter description

```
{
   "sensor_hostname": "os-992029000159.local",
   "data_destination": "169.254.240.233",
   "lidar_mode":"1024x20",
   "green_XY": [1, 2],
   "yellow_XY": [0.75, 1.5],
   "red_XY": [0.5, 1.0],
   "range_Z": [-0.7, 1.0]
}
```

Figure 2 Configure file of RPS platform.

Definitions of all the pins are shown in the following table. (Connector used here is 15EDGkm-3.81 mm with flange terminal. Pin numbers are one to six from right to left).

Definition of the connector is summarized in Table 2.

Figure 3 Connector of the RPS platform

Table 2 Definition and description of the RPS platform's connector

No.	IO	Explanation
1	VCC	5-24 V DC power input
2	GND	Ground
3	OUT1	Output interface 1 (corresponding to the green light), output VCC high level when obstacles are detected
4	OUT2	Output interface 2 (corresponding to the yellow light), output VCC high level when obstacles are detected

5	OUT3	Output interface 3 (corresponding to the red light), output VCC high level when obstacles are detected
6	GND	Pay attention to the ground wire of power supply

2.2 Jetson AGX based system

An orchard robot with sensor kit including GNSS-RTK positioning system, 3D LiDAR, 2D LiDAR and IMU is employed to verify the algorithm proposed in this paper as shown in Figure 1. The orchard robot chassis is 2 motor-driven kinematic system.

Table 3 Detailed information of 3D LiDAR, IMU and Encoder

	Parameter	Value
AGX	AI performance	32TOPS
	CPU	64-bits 8 core NVIDIA Carmel Arm
	GPU	64 Tensor cores NVIDIA Volta GPU
GNSS-RTK	Satellites	BDS GPS GLONASS GALILEO
	Antenna	4-frequency
	Precision	RTK mode 2 cm
	Communication	CAN
Lidar	Precision	±0.7-5 cm
	Frequency	10 Hz
	Detection distance	120 m
	Horizontal resolution	1024
IMU	Roll and pitch accuracy	0.25°
	Heading accuracy	1°
	Frequency	100 hz
Encoder	Resolution	1000P/R
	Frequency	100 hz

Experiments were implemented in both indoor and out environments to verify the proposed obstacle detection system. Indoor experiments were implemented on the RPS while the outdoor experiments were implemented on the AGX based system in the vineyard on an autonomous robot. The vineyard is in Zibo City, Shandong Province. Weeds and vines in the vineyard are regularly pruned, so Robot Perception and navigation are not affected. In order to facilitate the robot to have good traffic capacity in special environment such as muddy environment, the robot was designed with crawler chassis and driven by server motors.

Considering that the grapevine stalk point cloud above 0.5 m from the access road is relatively clean and less affected by weeds. The lidar was installed in the middle of the front end of the robot chassis, with a height of about 1.0 m from the ground, to adopt point cloud data more than 0.5 m from the ground.

The autonomous navigation system, worked as the main processor part of the robot, is used to process the 3D LiDAR cloud point information, to implement the navigation algorithms, and to manage the navigation information. The architecture of the navigation system is shown in Figure 4. The navigation controller is composed of a main processor NVIDIA Jetson AGX Xavier and an auxiliary processor embedded STM32F429 micro-controller.

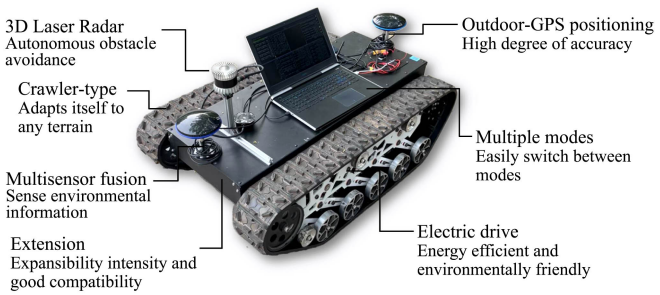

Figure 4 Description of the orchard robot and the sensors kit

The main processor AGX is used to run the Robot Operating System and 3D point cloud processing algorithms. The main processor is also used to connect to the LCD screen and the keyboard. The auxiliary processor is used to control the motors, to read the encoder data. Serial port is used to communicate in between the main processor and the auxiliary processor.

Multiple sensors are synchronized based on the time of the 3D LiDAR. When the controller obtains the LiDAR data through the network port, the odometer data of other sensors under the point cloud time is obtained by linear interpolation. The point cloud is registered by odometer data, and then the point cloud registration is optimized by Normal-Distribution Transformation (NDT). Then two lines are fitted by Random Sample Consensus (RANSAC) method based on the least square method, and the lines are filtered by EKF algorithm with the odometer calculated before as the input value.

Figure 5 The robot collects three-dimensional point clouds in the vineyard with a running person at the front of the moving robot

2.3 Obstacle detection methodology

The obstacle detection methodology proposed in this paper is based on 3D LiDAR point cloud while passthrough filter was employed to filter the point cloud map. After processing, the output binary signal is used into the orchard robot control system to start or stop the motivation of the orchard robot. The whole methodology is only added the software cost and computational cost without increasing the hardware cost which is usually very expensive.

The proposed obstacle detection algorithm is based on the passthrough filter. Passthrough filter is one of the helpful filters in ROS packages, which is used to cut off values that are either inside or outside a given user range. The range is usually given by experience. In our system, the maximum distance of the detectable is 7 m and the least distance is 0.7 m. These parameters are determined by the 3D-LiDAR and the mounted height of it.

The orchard environments are complex such as uneven soil road and weeds with different heights. In addition, due to the

different planting methods, the trees are planted long, resulting in a local area that is not a flat plane. Therefore, it is difficult to use the ground separation algorithm of hardened pavement to separate the soil ground. Here, the method of passthrough filtering is directly adopted in this paper, and the segmentation height is set according to experience to separate the orchard ground as a whole.

The proposed obstacle detection methodology is performed in three different steps summarized as follows. First, create the point cloud object to be processed, and store the point cloud object after the point cloud processing is completed. Then, set the capacity of the point cloud by width+height+length. After that, set the 'xyz' coordinates of all points in the point cloud and create a Passthrough Filter object and set its filtering parameters to filter the point cloud object to be processed as the input of the filter. Finally, result is obtained that the points within the range of x, y, and z set by the filter object will be retained, and the points outside the range will be discarded to realize the function of pass-through filtering.

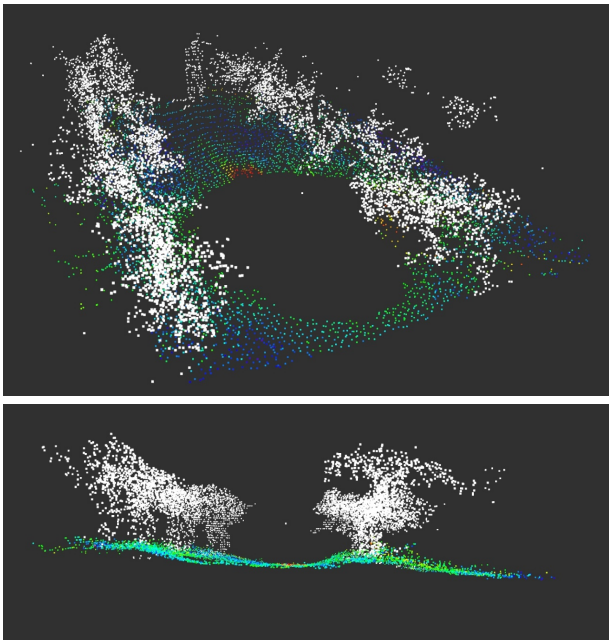

Figure 6 Passthrough filtering the point cloud data collected by the 3D-LiDAR

When the unmanned operation vehicle in the vineyard is planning to avoid obstacles, it only needs to plan the plane path, and does not need to plan the height direction. However, obstacles at different heights may still hinder the passage of the unmanned operation vehicle. Therefore, during the obstacle detection process It is necessary to detect the spatial range of the road for unmanned vehicles. In the planning path, if there is one more datum of height dimension, the calculation amount of path planning will increase sharply. Therefore, the obstacle data is dimensionally reduced, and its xyz three-dimensional data is compressed into the xy plane, as shown in the following figure.

From Figure 7 it is easy to see that the dimension reduced gird map is much smaller than the 3-dimentional point cloud map. And the obstacles in both the 2-dimentional point cloud map and 3-dimentional point cloud map were positioned at the same place in the map. It means that the distance in-between the obstacles and the moving robot had not been changed by the dimensionality reduction and compression. But the data size of the point cloud map had be greatly reduced by data compression that is why the computational complexity and computational cost have been reduced greatly. With several experiments, we have obtained that the maximum process time for each frame of the point cloud is less than 100 ms.

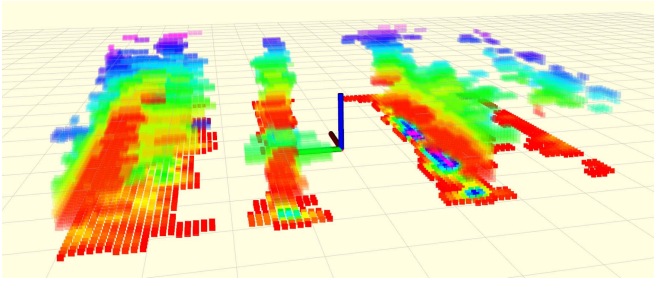

Figure 7 Data dimensionality reduction and compression

4 Results and discussion

To verify the proposed obstacle detection algorithm based on the passthrough filter, indoor and outdoor experiments are implemented with different parameters.

4.1 Indoor experiments

7 sets of experiments had been implemented under indoor environments to verify the ROI of the robot with the RPS platform. From Figure 8, we can see that when the 3D-LiDAR mounted with different heights, the scanning angle of the ROI ranged from –15 degrees to 15 degrees. Each grid is 5 degrees. Form sub-Figure8a to 8g, we can obtain that when the distance in-between the moving robot and obstacles is less than 2 m, the point cloud recognition result is not so good with too many points. Almost all different mounted height of the 3D-LiDAR except the 2.1 m on shown in Figure 8g, the curve converges quickly when the distance is greater than 2 m. Under this condition, the quantity of points in the point cloud map almost less than 1500. It will greatly increase the process speed. From Figure 8a to Figure 8g, we can obtain that for our vineyard robot, we should mount the 3D-LiDAR with the height of 1.5 m and the ROI should be set to be 0.7 m to 10 m to get the best result of obstacle detection and lowest computational cost.

4.2 Outdoor experiments

To verify the whole system with the autonomous navigation parts, the RPS platform is rewritten with in the ROS system as a separate function package. The functional package is incorporated into the autonomous system to verified in vineyard. From the experiments results summarized in the following table we can draw the conclusion that the proposed obstacle detection system based on the passthrough filter can successfully identify the obstacles in the front of the moving robot. Response time of the system is as low as 80 ms. The broke distance is around 1 m with a moving speed of 1 m/s.

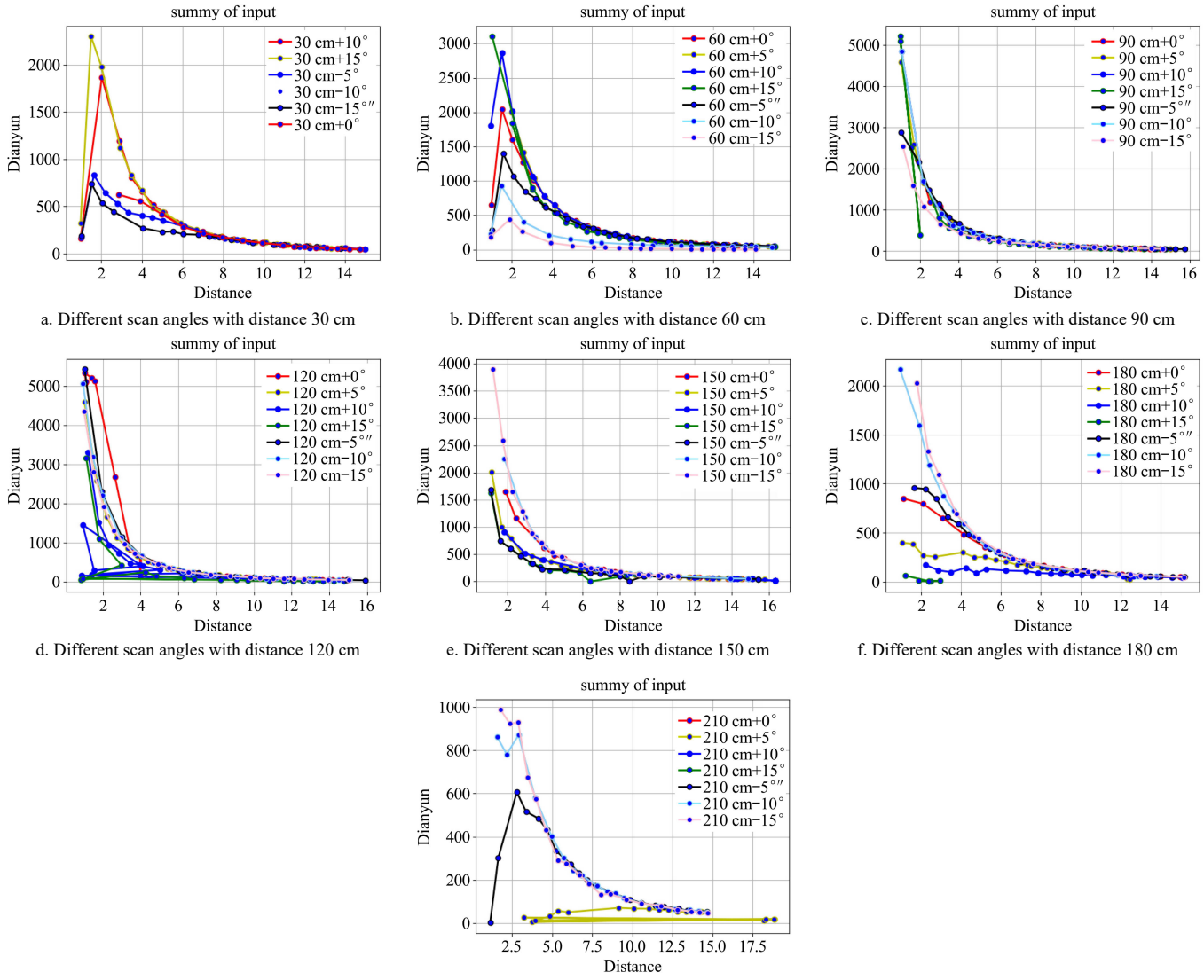

a. Different scan angles with distance 30 cm

b. Different scan angles with distance 60 cm

c. Different scan angles with distance 90 cm

d. Different scan angles with distance 120 cm

e. Different scan angles with distance 150 cm

f. Different scan angles with distance 180 cm

g. Different scan angles with distance 210 cm

Figure 8 Indoor experiment results with RPS platform. Form (a) to (g), different heights of the 3D-LiDAR are mounted on the moving robot to obtain the results of obstacles detection with different scanning angles

5 Conclusions

This paper has proposed a passthrough filter based obstacle detection algorithm. The algorithm is implemented on both the RPS platform and the Jetson AGX platform with ROS architecture. Indoor and outdoor experiments demonstrated that the real-time algorithm could successfully detect the obstacles in the front of the moving robot with low computational cost as low as 80 ms. Also we conclude that the best ROI range of our robot is 0.7 m to 10 m. Based on experiments results we also draw the conclusion that the best mounted height of our robot is around 1.5 m. To further expand our research results, we will test our system on different agriculture robots with different heigh and also test different 3D-LiDAR from different brands with different scanning angles. Except that, we also pay attention on the obstacle detection and local path planning incorporation algorithm to let the moving robot without stopping encounter small obstacles in front of it.

[References]

[1] Moorehead S, Wellington C, Gilmore B, Vallespi C. Automating Orchards: A System of Autonomous Tractors for Orchard Maintenance. In: Proceedings of International Scientific Conference. 2012 IEEE/RSJ International Conference on Intelligent Robots and Systems (IROS), 2012.

[2] Abe Y, Kamiya K, Osaki T, Kawano R, Miki N, Takeuchi S. Proceedings of the IEEE International Conference on Micro Electro Mechanical Systems (MEMS). In: Proceedings of International Scientific Conference "IEEE International Conference on Micro Electro Mechanical Systems", 2007.

[3] Wendeberg J, Schindelhauer C. Polynomial-time approximation algorithms for anchor-free TDoA localization. Theoretical Computer Science, 2014, 553: 27–36. doi: 10.1016/j.tcs.2014.04.007.

[4] D. Gonzlez, J. Prez, V. Milans, and F. Nashashibi, "A review of motion planning techniques for automated vehicles," IEEE Trans. on Intelligent Transportation Sys., vol. 17, no. 4, pp. 1135–1145, 2016.

[5] D. Droeschel, M. Nieuwenhuisen, M. Beul, D. Holz, J. Stuckler, and S. Behnke, "Multi-layered mapping and navigation for autonomous micro aerial vehicles," Journal of Field Robotics, vol. 33, no. 4, pp. 451–475, 2016.

[6] S. Scherer, S. Singh, and L. Chamberlain, "Flying fast and low among obstacles: Methodology and experiments," The International Journal of Robotics Research, vol. 27, no. 5, pp. 549–574, 2008.

[7] Yi L L, Sirajudeen G R, Lin Z P, See C M. Target tracking in mixed LOS/NLOS environments based on individual TOA measurement detection. IEEE Transactions on Wireless Communications, 2014, 13(1): 99–111.

[8] Zhao S, Chen Y M, Jay A F. High-Precision Vehicle Navigation in Urban Environments using a Low-cost Single-frequency RTK GPS Receiver. In: Proceedings of International Scientific Conference "2013 IEEE/RSJ International Conference on Intelligent Robots and Systems (IROS)", 2013. doi: 10.1109/TITS.2016.2529000.

[9] Jasurbek K, Park Y, Aamir S M. Survey of NLOS identification and

error mitigation problems in UWB-based positioning algorithms for dense environments. annals of telecommunications, 2010, 65(5): 301–311. doi: 10.1007/s12243-009-0124-z.

[10] Andrew B D, Gregory P A. Advances in animal ecology from 3D-LiDAR ecosystem mapping. Trends in Ecology & Evolution, 2014, 29(12): 681–691. doi: 10.1016/j.tree.2014.10.005.

[11] Hu J S, Wang J J, Daniel M H. Design of Sensing System and Anticipative Behavior for Human Following of Mobile Robots . in 2014 IEEE Transactions on Industrial Electronics, 2014, 61(4): 1916–1927. doi: 10.1109/TIE.2013.2262758.

[12] Zhang J, Andrew D C, Silvio M M, Marcel B, Sanjiv S. 3D perception for accurate row following: Methodology and results. In: Proceedings of International Scientific Conference "2013 IEEE/RSJ International Conference on Intelligent Robots and Systems, 2013: 5306-5313. doi: 10.1109/IROS.2013.6697124.

[13] Kong H, Jean Y A, Jean P. General Road Detection From a Single Image. in IEEE Transactions on Image Processing, 2010, 19(8): 2211–2220. doi: 10.1109/TIP.2010.2045715.

[14] Zhang X Y, Liu P B, Zhang C X. An Integration Method of Inertial Navigation System and Three-Beam Lidar for the Precision Landing. Mathematical Problems in Engineering, 2016: 1–13. doi: 10.1155/2016/4892376.

[15] Paul D G. Principles of GNSS, inertial, and multisensor integrated navigation systems. in IEEE Aerospace and Electronic Systems Magazine 2015, 30(2): 26–27. doi: 10.1109/MAES.2014.14110.

[16] Han H Z, Wang J, Wang J J, Tan X L. Performance Analysis on Carrier Phase-Based Tightly-Coupled GPS/BDS/INS Integration in GNSS Degraded and Denied Environments. Sensors, 2015, 15(4): 8685–8711. doi: 10.3390/s150408685.

[17] Liu L, Tao M, Niu R X, Wang J, et al. RBF-Based Monocular Vision Navigation for Small Vehicles in Narrow Space below Maize Canopy. Applied Sciences, 2016; 6(6):182. doi: 10.3390/app6060182.

[18] Neda N, Rene J L, Cheng J H, Denis G. A New Technique for Integrating MEMS-Based Low-Cost IMU and GPS in Vehicular Navigation. Journal of Sensors, 2016, 2016(4): 1–16. doi: 10.1155/2016/5365983.

[19] Lan Y B, Geng L J, Li W H, Ran W X, Yin X, Yi L L. Development of a robot with 3D perception for accurate row following in vineyard. Int J Precis Agric Aviat, 2021; 4(2): 14–21.

[20] Beau T, Lee D J, Kirt D L, James K A. Review of stereo vision algorithms and their suitability for resource-limited systems. Journal of Real-Time Image Processing, 2016, 11(1): 5–25. doi: 10.1007/s11554-012-0313-2.

[21] Jaemin B, Beom S S, Lee J H. Toward Accurate Road Detection in Challenging Environments Using 3D Point Clouds. ETRI Journal, 2015, 37(3): 606–616. doi: 10.4218/etrij.15.0113.1131.

[22] Naoum T, Dimitrios B, Dionysis B. AgROS: A Robot Operating System Based Emulation Tool for Agricultural Robotics. Agronomy, 2019, 9(7): 403. doi: 10.3390/agronomy9070403.

[23] Björn Å, Albert J B. A vision based row-following system for agricultural field machinery. Mechatronics, 2006, 15(2): 251–269. doi: 10.1016/j.mechatronics.2004.05.005

[24] Satow T, Matsuda K, Ming S B, Hironaka, K, Tan D. Development of laser crop row sensor for automatic guidance system of implements. In: Proceedings of International Scientific Conference Automation Technology for Off-road Equipment Conference, 2004. doi: 10.13031/2013.17826.

[25] Biber P, Ulrich W, Albert, A. Navigation system of the autonomous agricultural robot bonirob. In: Proceedings of International Scientific Conference 2012 IEEE/RSJ International Conference on Intelligent Robots and Systems, 2012.

[26] Pieter M B, Koen V B, Frits K V E, Joris I, Gook H K. Robot navigation in orchards with localization based on Particle filter and Kalman filter. Computers and Electronics in Agriculture, 2019, 157: 261–269. doi: 10.1016/j.compag.2018.12.046

[27] Zhang S, Guo C Y, Gao Z N, Adilet S, Chen J. Research on 2D Laser Automatic Navigation Control for Standardized Orchard. Applied Sciences, 2020, 10(8): 2763. doi: 10.3390/app10082763.

[28] Li Y W, Wang X J, Liu D X. 3D Autonomous Navigation Line Extraction for Field Roads Based on Binocular Vision. Journal of Sensors, 2019, 2019(8): 1–16. doi: 10.1155/2019/6832109.

[29] Bruna P P, Jose P M. Path errors in sugarcane transshipment trailers. Engenharia Agrícola, 2020, 40(2): 223–231. doi: 10.1590/1809-4430-Eng.Agric.v40n2p223-231/2020.

[30] Lyu H K, Park C H, Han D H, Kwak S, Choi B. Orchard Free Space and Center Line Estimation Using Naive Bayesian Classifier for Unmanned Ground Self-Driving Vehicle. Symmetry, 2018, 10(9): 1–14. doi: 10.3390/sym10090355.

[31] Hao Z, Xiong H L, Liu Y, Tan N D, Chen L. Trajectory Planning Algorithm of UAV Based on System Positioning Accuracy Constraints. Electronics, 2020, 9(2): 250. doi: 10.3390/electronics9020250.

[32] Sebastian T. Fox D. Probabilistic Robotics. Communications of the ACM, 2002, 45(3): 52–57. doi: 10.1145/504729.504754.